Radboud Repository

Radboud University Nijmegen

PDF hosted at the Radboud Repository of the Radboud University Nijmegen

Electronic, Magnetic and Transport Properties of Graphene Ribbons Terminated by Nanotubes

M. A. Akhukov, Shengjun Yuan[1], A. Fasolino and M. I. Katsnelson

Radboud University of Nijmegen, Institute for Molecules and Materials, Heijendaalseweg 135, 6525 AJ Nijmegen, The Netherlands

E-mail: [1]`s.yuan@science.ru.nl`

Abstract.
We study by density functional and large scale tight-binding transport calculations the electronic structure, magnetism and transport properties of the recently proposed graphene ribbons with edges rolled to form nanotubes. Edges with armchair nanotubes present magnetic moments localized either in the tube or the ribbon and metallic or half-metallic character, depending on the symmetry of the junction. These properties have potential for spin valve and spin filter devices with advantages over other proposed systems. Edges with zigzag nanotubes are either metallic or semiconducting without affecting the intrinsic mobility of the ribbon. By varying the type and size of the nanotubes and ribbons offers the possibility to tailor the magnetic and transport properties, making these systems very promising for applications.

The atomic structure of graphene edges is important for the determination of the electronic and magnetic properties of graphene, especially for narrow graphene nanoribbons[1, 2, 3, 4, 5, 6, 7, 8, 9, 10, 11, 12]. Recent theoretical work[13] on the stability of different graphene edges structures has shown that graphene edges can fold back on themselves and reconstruct as nanotubes, with low formation energy (see atomic structures in figure 1). In this article, we show that, beside protecting the edges from contamination and reconstructions, nanotubes at the edges may lead to magnetism and are not detrimental for the electronic mobility despite the row of sp^3 hybridized atoms at the ribbon-tube junction. We study the electronic and magnetic properties of these systems by a combination of density functional theory (DFT) and large scale tight binding (TB) simulations of transport properties. Our calculations suggest that these systems could be used for a variety of applications that we sketch in figure 2.

We consider systems formed by a nanoribbon terminated on both sides by the same armchair (AC) or zigzag (ZZ) nanotube. We notice that a ribbon with AC edges is terminated by ZZ nanotubes and a ribbon with ZZ edges is terminated by AC nanotubes. Nanoribbons terminated by AC nanotubes present interesting magnetic properties. By rolling the ZZ edges of a nanoribbon, two types of AC nanotubes can be formed, as shown in figure 1. If the atoms at the nanoribbon ZZ edge scroll and bind to the same sublattice sites within the nanoribbon, the formed AC nanotube has

Edges with armchair nanotube
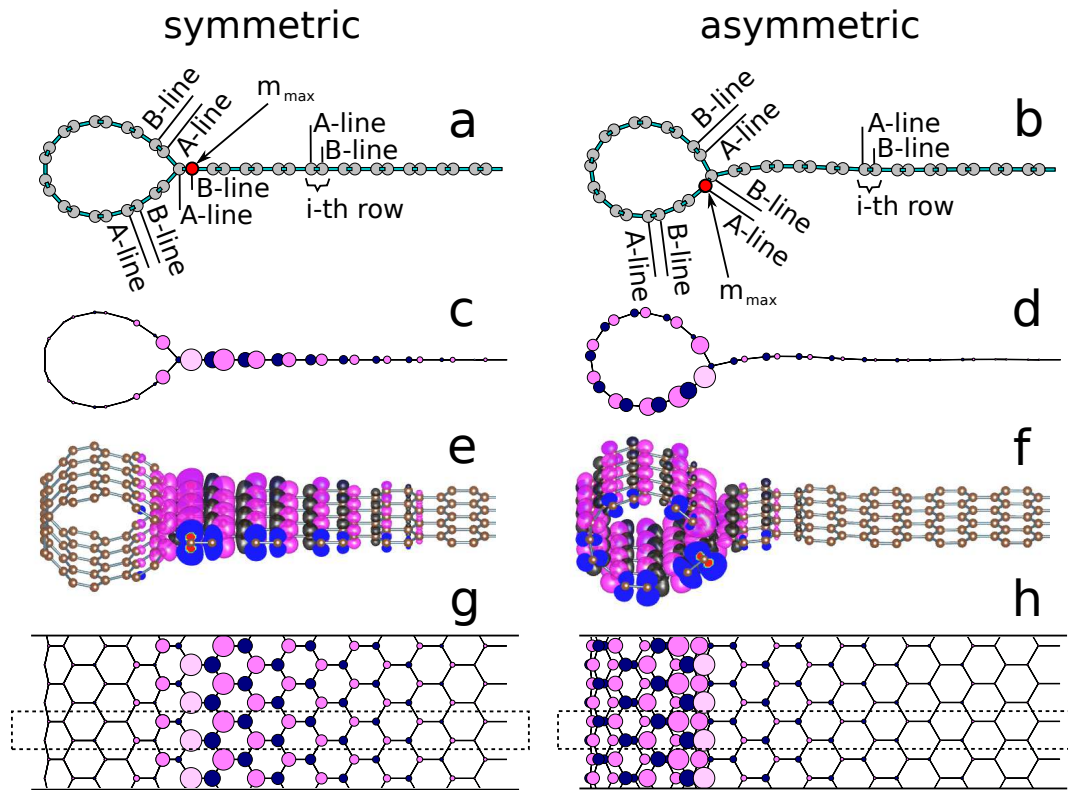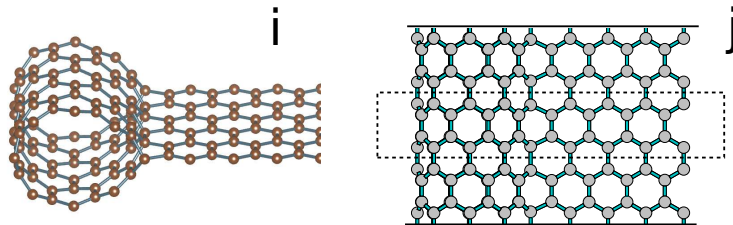
symmetric

asymmetric

Figure 1. (a-h) Structure and spin density for symmetric (left) and asymmetric (right) AC nanotube terminated edges. (a,b) Atomic structure; (c,d) Side, (e,f) 3D and (g,h) top view of schematic spin representation. The box with dashed line in (g,h) indicates half of the unit cell in the DFT calculation. For the symmetric case, the contribution to the magnetic moment from atoms belonging to the A- and B- sublattices are $m_A = 0.958$ μ_B and $m_B = -0.217$ μ_B (per half unit cell), and for the asymmetric case $m_A = 1.048$ μ_B and $m_B = -0.300$ μ_B. The maximum of the magnetic moment is located on the atom indicated by the arrow with the value $m_{max} = 0.379$ μ_B in both symmetric and asymmetric cases. (i,j) 3D and top view of AC nanoribbons terminated by ZZ nanotubes. The box with dashed line in (j) indicates half of the unit cell in the DFT calculation.

Table 1. Total spin magnetization S (in unit of μ_B per unit cell) as a function of the index of AC nanotube (N, N) and size of nanoribbon P (in unit of ZZ rows). The results in this table are for samples obtained by rolling the edges of the same unrolled graphene ribbon with width of 40 ZZ rows.

N	P	S (symmetric)	S (asymmetric)
9	4	0.000	1.499
8	8	0.995	1.499
7	12	1.371	1.499
6	16	1.481	1.499
5	20	1.500	1.500
4	24	1.500	1.500
3	28	1.494	1.500

mirror symmetry with respect to the nanoribbon plane; if the bonding sites belong to opposite sublattice, there is no such kind of symmetry (compare figure 1b to figure 1a). We call these two cases *symmetric* and *asymmetric* which corresponds to *armchair* and *armchair-like* in Ref. [13], respectively. The common point of these two cases is that the sublattice symmetry is broken, because all the sp^3 hybridized carbon atoms at the junction belong to one sublattice. Due to Lieb theorem [8, 12], this gives the possibility of spin polarization around the junctions. Since the theorem applies to the Hubbard model, accurate calculations for the real system are necessary to investigate this possibility.

In order to study the magnetic properties, we performed spin polarized DFT calculations by SIESTA[14, 15, 16]. We used generalized gradient approximation with Perdew-Burke-Ernzerhof parametrization (GGA-PBE) [17] and a standard built-in double-ζ polarized (DZP) [18] basis set to perform geometry relaxation. We found that, in both symmetric and asymmetric cases, there is spin polarization near the ribbon-tube junction, i.e., near the sp^3 hybridized carbon atoms. Note that the bond distance of these four-fold coordinated atoms is 1.54 Å like in diamond. The spin polarization is mainly located in the nanoribbon for the symmetric case and within the tube for the asymmetric case (see the isosurface plot of the spin density together with its symbolic representation in figure 1c-h). The up/down spins are distributed over the A/B sublattices respectively. The label m_{max} indicates the atom with the highest magnetic moment.

For the symmetric case, the value of the spin polarization increases with increasing nanoribbon width, and saturates at 1.50 μ_B per unit cell, when the nanoribbon width is wider than 16 ZZ rows; For the asymmetric case, the spin polarization is always 1.50 μ_B per unit cell, irrespective of the nanoribbon width and nanotube radius (see Table 1).

For the asymmetric case the spins are located inside the two nanotubes and therefore the exchange interaction between opposite edges is negligible. For the symmetric case, the spins on the two edges are coupled antiferromagnetically, similarly to hydrogen
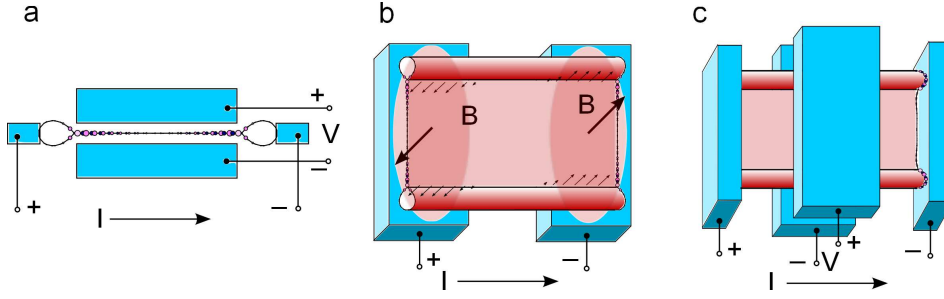
Figure 2. Sketch of spintronics devices based on carbon nanoribbons terminated by AC nanotubes. (a) A spin valve based on the symmetric case: a gate can be used to switch from the antiferromagnetically coupled state to the ferromagnetically coupled excited state, favouring spin transport from one nanotube to the other across the ribbon. (b) For both symmetric and asymmetric case, high magnetoresistance could be achieved by applying magnetic fields of different sign at the ends of the nanoribbons, as proposed in [19] for ZZ nanoribbons. (c) For the asymmetric case, a gate along the ribbon could be used to switch between two half-metallic energy regions to realize either a spin filter or a spin valve.

terminated graphene edges[20, 21]: for the structure shown in figure 1a, the energy of antiparallel spin configurations is 22 meV per unit cell (see figure 1g) lower than for parallel configurations. This sizeable coupling across the ribbon makes the symmetric systems promising as spin valve devices[22]. In figure 2a we show a configuration similar to that proposed for dumbbell graphene structures on the basis of the Hubbard Hamiltonian in the mean field approximation[23]. A gate could be used to bring the system from the antiferromagnetically coupled state to the ferromagnetically coupled excited state, favouring spin transport from one nanotube to the other across the ribbon. Moreover, both for the symmetric and asymmetric case, the magnetic moments along the ribbon-tube junction are qualitatively similar to the case of ZZ edges of nanoribbons. Therefore, high magnetoresistance could be expected, as proposed in [19] for nanoribbons with ZZ edges, by applying magnetic fields of different sign at the ends of the nanoribbon. A sketch of this device for our systems is shown in figure 2b.

The spin polarized density of states (DOS) reveals other features of interest for spintronics related to half-metallic character. In figure 3a and 3b we show the spin polarized DOS for the symmetric and asymmetric case respectively. We see that the symmetric case is metallic for both spins in the whole range of energy. The asymmetric case, instead, is a half-metal near the Fermi energy E_F, namely it is metallic for spin up and insulating for spin down. The half-metallic character of our systems provides opportunities as spin filters without the need of external electric fields[24], magnetic fields[25], ferromagnetic strips[26], impurities[27, 28, 29] or defects[30, 31]. Furthermore, there is the opposite half-metallic character at higher energies. Around 0.4 eV, there is insulating character for spin up and metallic character for spin down. As sketched in figure 2c, a gate along the ribbon could be used to switch between these two half-metallic energy regions and affect selectively the spin transport.
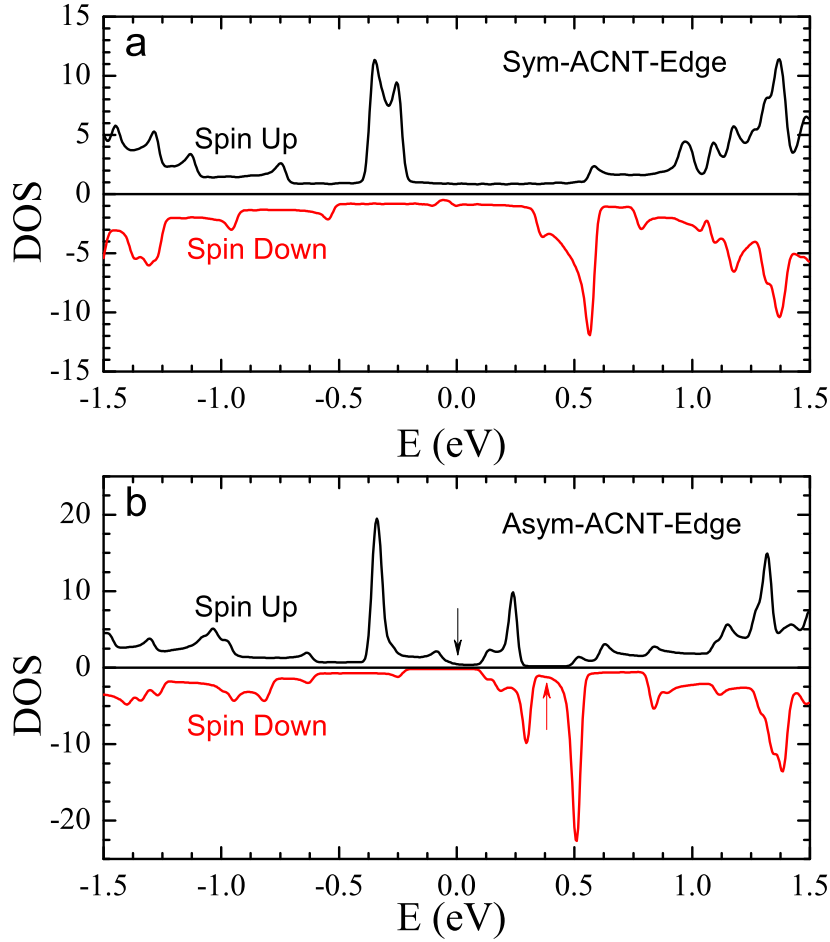
Figure 3. Density of states calculated by DFT for ZZ nanorribons with (a) symmetric and (b) asymmetric AC nanotube terminated edges ($N = 5$ and $P = 20$ for both cases). The arrows in (b) indicate the half-metalic energy regions for either spin up or spin down.

We come now to the case with ZZ nanotubes shown in figure 1i-j. For this case, there is only one type of ribbon-tube junction that preserves sublattice symmetry implying that there is no magnetization nor midgap states[8, 12]. The electronic structure and transport properties, however, strongly depend on the AC ribbon width and on the ZZ tube radius. In TB models, a AC nanoribbon is metallic if the number of AC rows is equal to $3l + 2$, where l is a positive integer, and semiconducting otherwise[1, 32]. Furthermore, ZZ nanotubes are metallic for index equal to $3l$[33]. In more general models, the properties of AC nanoribbons and ZZ nanotubes may differ from the ones predicted by TB, due to possible self passivation of the edges for nanoribbons and for the $\sigma - \pi$ band mixing for small nanotubes[33]. By using DFT calculations, we found that our joined system becomes a semiconductor with a gap of the order of few hundreds meV if both nanoribbon and nanotube are semiconducting. The energy gap as a function of geometry is shown in figure 4. The size of the nanotube has to be large enough for the opening of a band gap (figure 4a). For the joined system with semiconducting ZZ
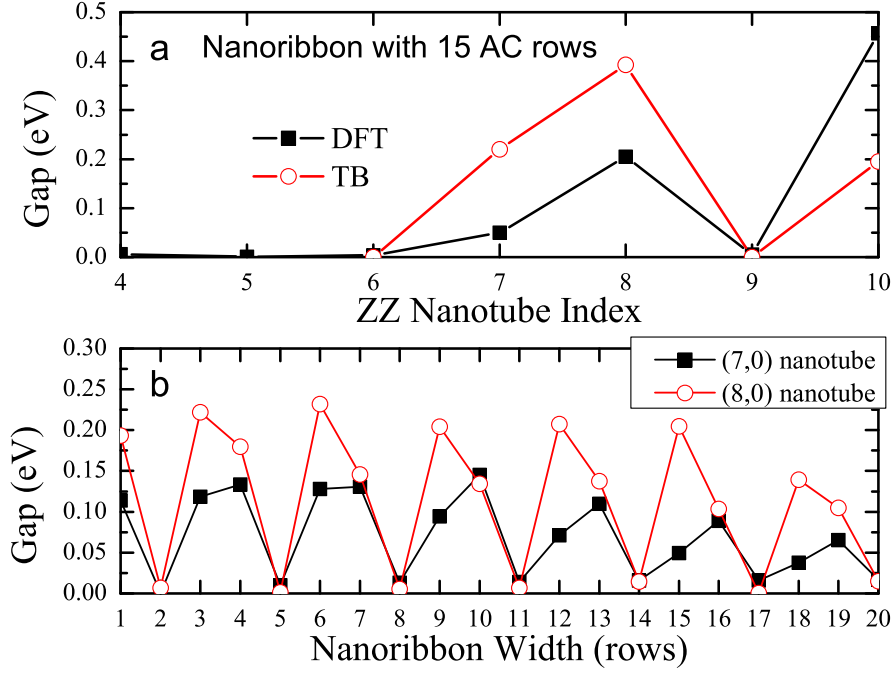
Figure 4. Band gap size-dependence in ZZ nanotube terminated AC nanoribbons. (a) Fixed nanoribbon with 15 AC rows for varying size of the terminating ZZ nanotube. (b) Fixed ZZ nanotube (8, 0 and 7, 0) edges for varying width of the AC nanoribbon.

nanotubes, there is a clear periodicity (3 ZZ rows) in the dependence of the energy gap on the nanoribbon width (figure 4b). For the studied cases, the value of the gap varies between 30 and 600 meV.

Since we want to calculate the transport properties by means of a simpler model, suitable for large samples, we have also calculated the energy structure of our system by π-band TB calculations where we consider only the nearest-neighbor hopping $t = 2.7$ eV between the carbon atoms[34, 35] for all bonds. The comparison between the gaps calculated by TB and DFT shown in figure 4a gives the same periodicity and a qualitative agreement. For the case of a AC nanoribbon with 15 rows terminated by (8,0) ZZ nanotubes we compare in figure 5a the TB and DFT DOS, which again are in qualitative agreement as to support the validity of the transport calculations we show next. The electronic transport properties of a semiconducting nanoribbon with or without nanotube terminated edges are obtained by using large scale TB simulations with about thirty million carbon atoms[34, 35]. In figure 5b we show that the electronic mobility parallel to the edges as a function of charge density are quite similar in these two cases. The mobility of the joined system is about 2250 $cm^2V^{-1}s^{-1}$ at charge density $n_e \sim 10^{13}cm^2$, which is only slightly smaller than the one of the AC nanoribbon at the same charge concentration.

In summary, we have studied the electronic and magnetic properties of graphene nanoribbons with three types of nanotube terminated edges. The spin magnetization is found to be 1.5 μ_B per unit cell in the ground state of both symmetric and asymmetric
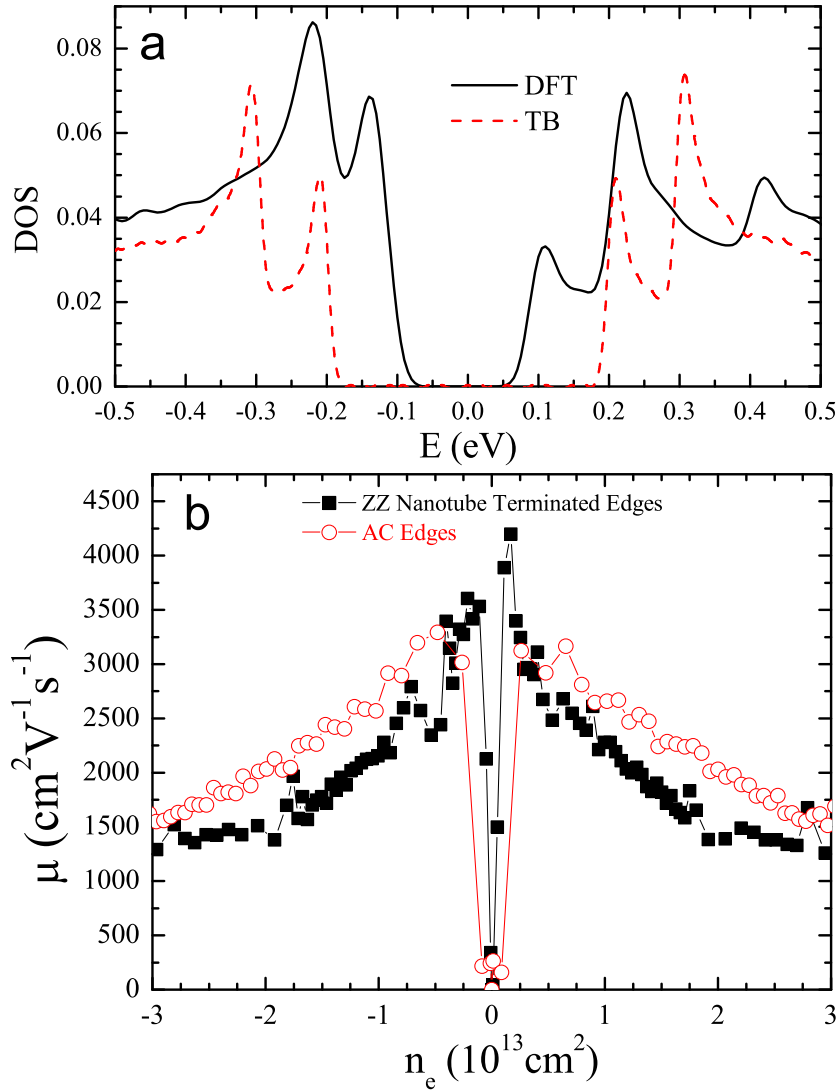
Figure 5. (a) Comparison of DOS of a nanoribbon with 15 AC rows terminated by (8,0) ZZ nanotubes calculated by DFT and TB. (b) Comparison of the mobility of a nanoribbon with 15 AC rows, terminated either by (8,0) ZZ nanotubes or by AC edges in TB. The charge density n_e is obtained from the density of state ρ in panel (a) by $n_e(E) = \int_0^E \rho(\epsilon)\,d\epsilon$. The sample contains 600000×47 carbon atoms for the case with ZZ nanotube terminated edges, and 2000000×15 for the case with AC edges.

AC nanotube terminated edges. For symmetric AC nanotube terminated edges, the spin density is located in the ribbon whereas, for the asymmetric case, it is located within the tube. In the ZZ nanotube terminated edges, there is a band gap opening of the order of few hundreds meV, if the constituent tube and nanoribbon are both semiconducting. The conductivity and mobility in the presence of ZZ nanotube terminated edges is comparable to the one of the AC nanoribbon itself.

Our calculations suggest that these systems are not only advantageous because the edges are protected against any kind of chemically induced disorder but also because,

by tailoring the ribbon/tube structure, they offer a wealth of possible applications for transport and spintronics.

Acknowledgments

References

[1] Son Y W, Cohen M L and Louie S G 2006 *Phys. Rev. Lett.* **97**(21) 216803
[2] Han M Y, Özyilmaz B, Zhang Y and Kim P 2007 *Phys. Rev. Lett.* **98**(20) 206805
[3] Koskinen P, Malola S and Häkkinen H 2008 *Phys. Rev. Lett.* **101**(11) 115502
[4] Wassmann T, Seitsonen A P, Saitta A M, Lazzeri M and Mauri F 2008 *Phys. Rev. Lett.* **101**(9) 096402
[5] Girit C O, Meyer J C, Erni R, Rossell M D, Kisielowski C, Yang L, Park C H, Crommie M F, Cohen M L, Louie S G and Zettl A 2009 **323** 1705–1708
[6] Liu Z, Suenaga K, Harris P J F and Iijima S 2009 *Phys. Rev. Lett.* **102**(1) 015501
[7] Wimmer M, Akhmerov A R and Guinea F 2010 *Phys. Rev. B* **82**(4) 045409
[8] Yazyev O V *Reports on Progress in Physics* **73** 056501
[9] van Ostaay J A M, Akhmerov A R, Beenakker C W J and Wimmer M 2011 *Phys. Rev. B* **84**(19) 195434
[10] Jia X, Campos-Delgado J, Terrones M, Meunier V and Dresselhaus M S 2011 *Nanoscale* **3**(1) 86–95
[11] Kunstmann J, Özdoğan C, Quandt A and Fehske H 2011 *Phys. Rev. B* **83**(4) 045414
[12] Katsnelson M I 2012 *Graphene: Carbon in Two Dimensions* (Cambridge University Press)
[13] Ivanovskaya V V, Zobelli A, Wagner P, Heggie M I, Briddon P R, Rayson M J and Ewels C P 2011 *Phys. Rev. Lett.* **107**(6) 065502
[14] Soler J M, Artacho E, Gale J D, Garcia A, Junquera J, Ordejon P and Sanchez-Portal D 2002 *J. Phys.: Condens. Matter* **14** 2745–2779
[15] Sanchez-Portal D, Ordejon P and Canadell E 2004 *Principles and Applications of Density functional Theory in Inorganic Chemistry II* 113 (Berlin: Springer)
[16] Artacho E, Anglada E, Dieguez O, Gale J D, Garcia A, Junquera J, Martin R M, Ordejon P, Pruneda J M, Sanchez-Portal D and Soler J M 2008 *J. Phys.: Condens. Matter* **20** 064208
[17] Perdew J P, Burke K and Ernzerhof M 1996 *Phys. Rev. Lett.* **77**
[18] Junquera J, Paz O, Sánchez-Portal D and Artacho E 2001 *Phys. Rev. B* **64**
[19] Kim W Y and Kim K S 2008 *Nature Nanotech.* **3** 408–412 ISSN 1748-3387
[20] Yazyev O V and Katsnelson M I 2008 *Phys. Rev. Lett.* **100**
[21] Bhandary S, Eriksson O, Sanyal B and Katsnelson M I 2010 *Phys. Rev. B* **82**
[22] Hill E W, Geim A K, Novoselov K, Schedin F and Blake P 2006 *IEEE Trans. Magn.* **42** 2694–2696 ISSN 0018-9464 41st IEEE International Magnetics Conference (Intermag 2006), San Diego, CA, MAY 08-12, 2006
[23] Ma Z and Sheng W 2011 *Appl. Phys. Lett.* **99**(8) 083101
[24] Son Y W, Cohen M L and Louie S G 2006 *Nature* **444** 347–349
[25] Abanin D A, Lee P A and Levitov L S 2006 *Phys. Rev. Lett.* **96**(17) 176803
[26] Zhang Y T, Jiang H, Sun Q f and Xie X C 2010 *Phys. Rev. B* **81**(16) 165404
[27] Hod O, Barone V, Peralta J E and Scuseria G E 2007 *Nano Lett.* **7** 2295–2299

[28] Zheng X H, Wang R N, Song L L, Dai Z X, Wang X L and Zeng Z 2009 *Appl. Phys. Lett.* **95**

[29] Soriano D, Muñoz Rojas F, Fernández-Rossier J and Palacios J J 2010 *Phys. Rev. B* **81**(16) 165409

[30] Martins T B, da Silva A J R, Miwa R H and Fazzio A 2008 *Nano Lett.* **8** 2293–2298

[31] Lisenkov S, Andriotis A N and Menon M 2012 *Phys. Rev. Lett.* **108**(18) 187208

[32] Ezawa M 2006 *Phys. Rev. B* **73**(4) 045432

[33] Dubois S M M, Zanolli Z, Declerck X and Charlier J C 2009 *Eur. Phys. J. B* **72**

[34] Wehling T O, Yuan S, Lichtenstein A I, Geim A K and Katsnelson M I 2010 *Phys. Rev. Lett.* **105** 056802

[35] Yuan S, De Raedt H and Katsnelson M I 2010 *Phys. Rev. B* **82** 115448